

**DEDICATED TO MY LOVING
BROTHER
VINAY...**

CERTIFICATE

It is certified that the work contained in the thesis titled “**Synergistic and compositional modulation of advanced transition metal oxide based electrocatalysts for alkaline water oxidation**” by **Sarvatej Kumar Maurya** has been carried out under my supervision and this work has not been submitted elsewhere for a degree.

It is further certified that the student has fulfilled all the requirements of Comprehensive Examination, Candidacy, and SOTA for the award of Ph. D Degree.

Date: 14/ May/2025
Place: Varanasi

Manisha Malviya

Dr. Manisha Malviya

(Supervisor)

Department of Chemistry,
Indian Institute of Technology
(Banaras Hindu University),

Varanasi-221005

Dr. MANISHA MALVIYA
DEPARTMENT OF CHEMISTRY
IIT (BHU), VARANASI
U.P.-221005

DECLARATION BY THE CANDIDATE

I, **Sarvatej Kumar Maurya**, certify that the work embodied in this thesis is my own bonafide work and carried out by me under the supervision of **Dr. Manisha Malviya** from **Dec-2018 to April-2025**, at the **Department of Chemistry, Indian Institute of Technology, (BHU), Varanasi**. The matter embodied in this thesis has not been submitted for the award of any other degree/diploma. I declare that I have faithfully acknowledged and given credits to the research workers wherever their works have been cited in my work in this thesis. I further declare that I have not willfully copied any other's work, paragraphs, text, data, results, etc., reported in journals, books, magazines, reports, dissertations, theses, etc., or available at websites and have not included them in this thesis and have not cited as my own work.

Date: 14/May/2025

Place: Varanasi

(Sarvatej Kumar Maurya)

CERTIFICATE BY THE SUPERVISOR

It is certified that the above statement made by the student is correct to the best of my/our knowledge.

Supervisor

Dr. Manisha Malviya
Department of Chemistry
Indian Institute of Technology
(Banaras Hindu University)
Varanasi- 221005

Co-supervisor

Prof. Dhanesh Tiwary
Department of Chemistry
Indian Institute of Technology
(Banaras Hindu University)
Varanasi- 221005

Head of Department

Prof. Sundaram Singh
Department of Chemistry,
Indian Institute of Technology
(Banaras Hindu University),
Varanasi- 221005

Dr. Manisha Malviya
DEPARTMENT OF CHEMISTRY
INDIAN INSTITUTE OF TECHNOLOGY
(B.H.U.)
VARANASI-221005

Dr. Dhanesh Tiwary
Professor
रसायन विज्ञान विभाग
Department of Chemistry
भारतीय प्रौद्योगिकी संस्थान (एन.ए.ए.ए.ए.)
Indian Institute of Technology (B.H.U.)
वाराणसी-221005/Varanasi-221005

विभागाध्यक्ष / HEAD
रसायन विज्ञान विभाग
Department of Chemistry
भारतीय प्रौद्योगिकी संस्थान (एन.ए.ए.ए.ए.)
Indian Institute of Technology (B.H.U.)
वाराणसी-221005/Varanasi-221005

COPYRIGHT TRANSFER CERTIFICATE

Title of the Thesis: **Synergistic and compositional modulation of advanced transition metal oxide based electrocatalysts for alkaline water oxidation.**

Name of the Student: **Sarvatej Kumar Maurya**

COPYRIGHT TRANSFER

The undersigned hereby assigns to the Indian Institute of Technology (Banaras Hindu University) Varanasi all rights under copyright that may exist in and for the above thesis submitted for the award of the "**Doctor of Philosophy**" degree.

Date: 14/May/2025

Place: Varanasi.



(Sarvatej Kumar Maurya)

Note: However, the author may reproduce or authorize others to reproduce material extracted verbatim from the thesis or derivative of the thesis for author's personal use provided that the source and the Institute's copyright notice are indicated.

Acknowledgement

It is indeed my proud privilege to express my deep sense of gratitude and indebtedness to my supervisor Dr. Manisha Malviya and my co-supervisor, Prof. Dhanesh Tiwary, Department of Chemistry, Indian Institute of Technology (BHU), Varanasi, for their enormous help, co-operation, and valuable supervision that they have extended to me for the successful completion of this investigation. I am indebted to them for their consistent encouragement, sustained interest, and parental care throughout the research period.

I am obliged very much to express my sincere thanks to HOD, Prof. Sundaram Singh, and former HOD, Prof. Y. C. Sharma, Department of Chemistry, IIT (BHU) for providing necessary facilities and constant motivation throughout my research work.

It is my pleasure to express my cheers to all RPEC members Dr. Arindam Indra, Department of Chemistry, IIT (BHU), and Dr. Bhavna Verma, Department of Chemical Engineering, IIT (BHU) for their valuable suggestions, constant guidance, and kind encouragement during my research work. They always came forward to assist me whenever I needed. I would also like to acknowledge Prof. Prabhakar Singh, Department of Physics, IIT (BHU), and Prof. Manoj Kumar Bharti, Department of Chemistry, (BHU), for providing instrumental facilities.

My passionate thanks go to all the faculty members, Department of Chemistry, IIT (BHU) for their support and encouragement.

I constraint special thanks to all non-teaching staff (Mr. Rambish, Neeraj, Abhishek, and Amit) of the Department of Chemistry, IIT (BHU) as this work would have never been completed without their technical support.

I also acknowledge the Ministry of Education (MoE), Government of India, New Delhi, and Director, IIT (BHU) for the financial support in the form of a teaching assistantship. I

gratefully acknowledge the facilities provided by CIF, IIT (BHU), Varanasi for various characterizations of samples.

I am blessed to have very supportive and caring labmates Dr. Neetu Verma, Ms. Amisha Soni, Dr. Manjit Singh, Dr. Kuldeep Kumar Maurya, Dr. Kulveer Singh, for their valuable support and encouragement towards the successful completion of my research work.

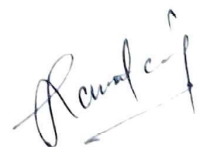
I would like to thank my friends, Dr. Ved Vyas, Dr. Uma Sharma, for their help and support.

I express my deepest affection to my loving mother Mrs. Usha Devi, caring father Mr. Surendra Pratap Maurya, brothers Mr. Sarvajeet Kumar Maurya and Lt. Mr. Sarvavijay Kumar Maurya (Vinay), sister Vandana Maurya, brother in law Mr. Pawan Kumar, and all my family members for their love, concern, continuous moral support and encouragement which enabled me to perform my liabilities.

At the last but not the least, I thank to all my well-wishers and critics whom names I may have failed to mention here unintentionally. Thanks to all, for being there for me when times were the toughest.

Date: 14/May/2025

Place: Varanasi



(Sarvatej Kumar Maurya)

List of Figures

Figure No.	Title	Page No.
Figure 1.1	(a) Annual global energy consumption, (b) fossil CO ₂ emission by fuel type (Coal oil and natural gas) and from cement production and flaring. (Global fossil carbon emissions rebound near pre-COVID-19 levels)	2
Figure 1.2	Flowchart illustrating the types of primary and secondary batteries	10
Figure 1.3	Pictorial representation of electrochemical water splitting	13
Figure 1.4	Plausible mechanism through AEM pathway	17
Figure 1.5	Plausible mechanism through LOM pathway	19
Figure 1.6	Schematic diagram of OPM pathway for OER	21
Figure 1.7	Parameters used to investigate electrocatalytic activity	25
Figure 2.1	(a) Image of FT-IR spectrometer, (b) Michelson interferometer's operating principle	46
Figure 2.2	(a) Image of Rigaku Miniflex 600 diffractometer, (b) schematic illustration of X-ray beam diffraction through a crystalline material	47
Figure 2.3	(a) Image of Raman Spectrophotometer, (b) schematic illustration of Raman scattering	49
Figure 2.4	(a) Image of FE-SEM instrument, (b) components of the instrument	50
Figure 2.5	(a) HR-TEM instrument, (b) schematic diagram illustrating the components of a TEM microscope	52
Figure 2.6	(a) BET instrument, (b) schematic diagram illustrating the components of Quantachrome Autosorb	56
Figure 2.7	Types of hysteresis loops classified by IUPAC	57
Figure 2.8	(a) XPS instrument, (b) schematic diagram illustrating the components of XPS system equipped with (Mg K α) non-monochromatic X-ray source	59
Figure 2.9	(a) CHI 608C electrochemical workstation, (b) electrochemical cell representation with a three-electrode setup	62
Figure 2.10	(a) Typical Cyclic Voltammogram, (b) CV in non-faradaic region	65
Figure 2.11	Nyquist plot and its fitted equivalent circuit	69

Figure 3.1	XRD patterns of a) BCTO, b) Mg _{0.05} BCTO, c) Mg _{0.1} BCTO and d) Mg _{0.2} BCTO catalysts	81
Figure 3.2	FT-IR spectra of a) BCTO, b) Mg _{0.05} BCTO, c) Mg _{0.1} BCTO, d) Mg _{0.2} BCTO catalyst	82
Figure 3.3	Raman spectra of Mg _{0.1} BCTO	83
Figure 3.4	Raman spectra of a) BCTO, b) Mg _{0.05} BCTO, c) Mg _{0.2} BCTO	84
Figure 3.5	a, b) SEM images of Mg _{0.1} BCTO at different magnifications, c) TEM image of Mg _{0.1} BCTO, d) HR-TEM image of Mg _{0.1} BCTO, e) SAED pattern, f) Particle size distribution of Mg _{0.1} BCTO with standard deviation	85
Figure 3.6	a) FE-SEM image of Mg _{0.1} BCTO, b) Corresponding EDS spectra	86
Figure 3.7	Elemental mapping of Mg _{0.1} BCTO	87
Figure 3.8	FE-SEM images of a) BCTO, b) Mg _{0.05} BCTO, c) Mg _{0.1} BCTO, d) Mg _{0.2} BCTO	88
Figure 3.9	EDS spectra and elemental mapping of BCTO ceramic material	89
Figure 3.10	EDS spectra and elemental mapping of BCTO ceramic material	89
Figure 3.11	High resolution of XPS spectra of a) Mg 1s, b) Bi 4f, c) Cu 2p, d) Ti 2p, e) O1s	91
Figure 3.12	a) LSV at a scan rate of 0.5 mV s ⁻¹ in 1 M KOH at 25 °C, b) Tafel slopes, c) Variation of overpotential with as prepared catalysts and bare electrode, d) CV of FTO/Mg _{0.1} BCTO electrode in non-faradaic region at different scan rates, e) Corresponding C _{dl} plot for FTO/Mg _{0.1} BCTO electrode f) Variation of Tafel slopes with as prepared catalysts and bare electrode	93
Figure 3.13	CV of prepared catalysts and bare electrode	94
Figure 3.14	a) Nyquist plots, b) Fitted Nyquist plot of FTO/Mg _{0.1} BCTO electrode	97
Figure 3.15	a) Comparative ECSA for all the prepared catalysts normalized by mass loading, b) Nyquist plots normalized by mass loading of the catalysts	98
Figure 3.16	Nyquist plots of FTO/Mg _{0.1} BCTO electrode on increasing potential	99

- Figure 3.17** a) CV of FTO/Mg_{0.2}BCTO electrode in non-faradaic region at different scan rates, b) Tafel polarization curves of FTO/Mg_{0.2}BCTO electrode at different temperatures, c) Tafel polarization curves of FTO/Mg_{0.2}BCTO electrode at different concentrations of KOH, d) Corresponding C_{dl} plot for FTO/Mg_{0.2}BCTO electrode, e) Corresponding Arrhenius plot for FTO/Mg_{0.2}BCTO, f) order of reaction for FTO/Mg_{0.2}BCTO electrode **99**
- Figure 3.18** a) CV of FTO/Mg_{0.05}BCTO electrode in non-faradaic region at different scan rates, b) Tafel polarization curves of FTO/Mg_{0.05}BCTO electrode at different temperatures, c) Tafel polarization curves of FTO/Mg_{0.05}BCTO electrode at different concentrations of KOH, d) Corresponding C_{dl} plot for FTO/Mg_{0.05}BCTO electrode, e) Corresponding Arrhenius plot for FTO/Mg_{0.05}BCTO electrode, f) order of reaction for FTO/Mg_{0.05}BCTO electrode **100**
- Figure 3.19** a) CV of FTO/BCTO electrode in non-faradaic region at different scan rates, b) Tafel polarization curves of FTO/BCTO electrode at different temperatures, c) Tafel polarization curves of FTO/BCTO electrode at different concentrations of KOH, d) Corresponding C_{dl} plot for FTO/BCTO electrode, e) Corresponding Arrhenius plot for FTO/BCTO electrode, f) order of reaction for FTO/BCTO electrode **101**
- Figure 3.20** a) CV of bare FTO electrode in non-faradaic region at different scan rates, b) Tafel polarization curves of bare FTO electrode at different temperatures, c) Tafel polarization curves of bare FTO electrode at different concentrations of KOH, d) Corresponding C_{dl} plot for bare FTO electrode, e) Corresponding Arrhenius plot for bare FTO electrode, f) order of reaction for bare FTO electrode **102**
- Figure 3.21** a) Tafel polarization curves of FTO/Mg_{0.1}BCTO electrode at different temperatures, b) Corresponding Arrhenius plot, c) Tafel polarization curves of FTO/Mg_{0.1}BCTO electrode at different concentrations of KOH d) order of reaction **104**
- Figure 3.22** Chronopotentiometry test at a constant current of 10 mA cm⁻² **106**

Figure 4.1	XRD patterns of (a) $\text{Co}_{0.5}\text{W}_{1.5}\text{O}_4$, (b) CoWO_4 , (c) $\text{Co}_{1.5}\text{W}_{0.5}\text{O}_4$	124
Figure 4.2	FT-IR of (a) $\text{Co}_{0.5}\text{W}_{1.5}\text{O}_4$, (b) CoWO_4 , (c) $\text{Co}_{1.5}\text{W}_{0.5}\text{O}_4$	126
Figure 4.3	Raman spectra of (a) $\text{Co}_{0.5}\text{W}_{1.5}\text{O}_4$, (b) CoWO_4 , (c) $\text{Co}_{1.5}\text{W}_{0.5}\text{O}_4$	127
Figure 4.4	a) TEM micrograph of CoWO_4 catalyst, b) SAED pattern of CoWO_4 , c) HR-TEM micrograph of CoWO_4 catalyst, d) particle size distribution of CoWO_4	129
Figure 4.5	High resolution XPS spectra of a) Co 2p, b) W 4f, c) O 1s	130
Figure 4.6	(a) LSV curves recorded at a scan rate of 0.5 mV s^{-1} in 1 M KOH at 25 °C, (b) Tafel slope analysis of the investigated catalysts, (c) comparison of overpotential values for the prepared catalysts, (d) CV of the FTO/ CoWO_4 electrode in the non-faradaic region at varying scan rates, (e) corresponding C_{dl} plot for the FTO/ CoWO_4 electrode, and (f) Tafel slope variation across the prepared catalysts	133
Figure 4.7	CV of prepared catalysts	134
Figure 4.8	$\text{Co}_{0.5}\text{W}_{1.5}\text{O}_4$: a) CV in non-faradaic region at different scan rates, b) Tafel polarization curves at different temperatures, c) Tafel polarization curves at different concentrations of KOH, d) corresponding C_{dl} plot, e) corresponding Arrhenius plot, f) order of reaction	135
Figure 4.9	$\text{Co}_{1.5}\text{W}_{0.5}\text{O}_4$: a) CV in non-faradaic region at different scan rates, b) Tafel polarization curves at different temperatures, c) Tafel polarization curves at different concentrations of KOH, d) corresponding C_{dl} plot, e) corresponding Arrhenius plot, f) order of reaction	136
Figure 4.10	(a) Nyquist plots, (b) fitted Nyquist plot of FTO/ CoWO_4 electrode, (c) chronopotentiometry test of the FTO/ CoWO_4 electrode, and (d) ECSA variation for the synthesized catalysts	140
Figure 4.11	(a) Tafel polarization plots of the FTO/ CoWO_4 electrode at various temperatures, (b) corresponding Arrhenius plot, (c) Tafel polarization plots of the FTO/ CoWO_4 electrode at varying KOH concentrations. (d) reaction order determination	142

Figure 5.1	XRD patterns of a) ppy, b) CoWO ₄ , c) CoWO ₄ /ppy composite	163
Figure 5.2	XRD patterns of CoWO ₄ /ppy composite material, a) before heating and b) after heating the sample	164
Figure 5.3	FT-IR of CoWO ₄ and CoWO ₄ /ppy composite	165
Figure 5.4	a) TEM micrograph of CoWO ₄ /ppy catalyst, b) magnified TEM micrograph of composite, c) HR-TEM micrograph of CoWO ₄ /ppy catalyst, d) SAED pattern of composite, e) Particle size distribution of composite	166
Figure 5.5	TEM micrographs of, a) pristine CoWO ₄ and b) CoWO ₄ /ppy	167
Figure 5.6	5.6. High resolution XPS spectra of a) Co 2p, b) W 4f, c) O 1s, d) C 1s, e) N 1s	169
Figure 5.7	a) The gas adsorption–desorption isotherm curve of CoWO ₄ /ppy and, b) inset shows the BJH plot for the porosity evolution of CoWO ₄ /ppy	171
Figure 5.8	a) LSV of prepared catalysts along with bare electrode at 0.5 mV s ⁻¹ scan rate in 1 M KOH electrolyte at 25 °C, b) Tafel slopes, c) Comparison of overpotential among the synthesized materials and the bare electrode, d) CV of FTO/CoWO ₄ /ppy electrode in non-faradaic region at varying scan rates, e) C _{dl} plot for FTO/ CoWO ₄ /ppy electrode f) Comparison of Tafel slopes among the synthesized materials and the bare electrode	172
Figure 5.9	High resolution XPS spectra of a) Co 2p, b) W 4f, c) O 1s	173
Figure 5.10	CV of prepared catalysts and bare electrode	174
Figure 5.11	CoWO₄: a) CV in non-faradaic region at different scan rates, b) Tafel polarization curves at different temperatures, c) Tafel polarization curves at different concentrations of KOH, d) corresponding C _{dl} plot, e) corresponding Arrhenius plot, f) order of reaction	175
Figure 5.12	a) CV in non-faradaic region at different scan rates, b) Tafel polarization curves different temperatures, c) Tafel polarization curves at different concentrations of KOH, d) Corresponding C _{dl} plot, e) Corresponding Arrhenius plot, f) order of reaction	176

- Figure 5.13** a) Nyquist plots of prepared catalysts and bare electrode at 1.3 V vs. RHE, b) Circuit fitted Nyquist plot of FTO/CoWO₄/ppy electrode, c) Chronopotentiometry stability test for FTO/CoWO₄/ppy electrode, d) Comparison of ECSA among the synthesized electrocatalysts and the bare electrode **180**
- Figure 5.14** a) Tafel plots of FTO/CoWO₄/ppy electrode at increasing temperatures from 25 °C to 55 °C, b) Arrhenius plot, c) Tafel plots of FTO/CoWO₄/ppy electrode at varying concentrations of KOH d) order of reaction **184**

List of Table

Table No.	Title	Page No.
Table 1.1	Classification of Fuel Cells and their operating parameters	5
Table 3.1	Electrode kinetic parameters	95
Table 3.2	Thermodynamic parameters	105
Table 4.1	Required stoichiometric amounts of metal precursors used for the synthesis of cobalt tungstate nanoparticles	120
Table 4.2	Electrode kinetic parameters	137
Table 4.3	Thermodynamic parameters	143
Table 5.1	Comparison of various parameters of electrocatalytic OER for transition metal based and hybrid materials reported in the literature	177
Table 5.2	Electrode kinetic parameters	178
Table 5.3	Thermodynamic parameters	186

List of Symbols/Abbreviations

C_{dl}	Double-layer capacitance
cm	Centimeter
CP	Chronopotentiometry
ECSA	Electrochemically active surface area
CV	Cyclic voltammetry
EDS	Energy dispersive spectroscopy
EIS	Electrochemical impedance spectroscopy
FTO	Fluorine doped tin oxide
HER	Hydrogen evolution reaction
HR-TEM	High-resolution transmission electron microscopy
iR	Internal resistance
FT-IR	Fourier transform infrared spectroscopy
kJ	Kilo joule
LSV	Linear sweep voltammetry
mA	Milli ampere
mV	Milli volt
OER	Oxygen evolution reaction
Oh	Octahedral
P-XRD	Powder X-ray diffraction
R_s	Solution resistance
R_{ct}	Charge transfer resistance
RHE	Reversible hydrogen electrode
RT	Room temperature
SAED	Selected area electron diffraction pattern
FE-SEM	Field emission-scanning electron microscopy
UV-Vis	Ultraviolet-visible
R_f	Roughness factor
μF	Micro farad
dec	Decade
Mj	Mega joule

kg	Kilo gram
$\Delta H_{el}^{0\ddagger}$	Standard electrochemical energy of activation
$\Delta S_{el}^{0\ddagger}$	Standard entropy of activation
$\Delta H^{0\ddagger}$	Standard enthalpy of activation
α	Transfer coefficient
GCE	Glassy carbon electrode
SEC	Spectro-electrochemistry
k_B	Boltzmann constant
h	Planck constant
C_{OH^-}	Hydroxyl ion concentration
R	Universal gas constant
b	Tafel slope
T	Temperature
F	Faraday constant
j	Joule
η_{10}	Overpotential at 10 mA cm ⁻² current density
NHE	Normal hydrogen electrode
η_1	Overpotential at 1 mA cm ⁻² current density